

# Role of Impurity Cyclotron Damping in Ion Heating and RFP Turbulence

P.W. Terry, V. Tangri, J.S. Sarff, G. Fiksel, A.F. Almagri, Y. Ren, and S.C. Prager

Department of Physics, University of Wisconsin-Madison, Madison, Wisconsin 53706

e-mail contact of main author: [pwterry@wisc.edu](mailto:pwterry@wisc.edu)

**Abstract:** In the reversed field pinch ions are heated anomalously relative to collisional energy exchange with Ohmically heated electrons. The process channels electron energy to ions in a way that is still not understood. Recent observations suggest that impurities are preferentially heated. A theory for ion heating via impurity ion-cyclotron-resonant damping of the turbulent energy cascaded from unstable global tearing modes is presented. The theory treats the magnetic turbulence as an Alfvén wave cascade and calculates the rate of damping to impurity ions via cyclotron resonances. The transient temperature rise in sawtooth crashes is modeled from a 0-D transport model that accounts for the resonant cyclotron heating, anomalous heat losses, and collisional equipartition between impurities, bulk ions, electrons, and parallel and perpendicular temperatures. The larger fluctuation level at lower impurity cyclotron frequencies and the multiplicity of impurity resonances lead to heating rates that are consistent with experiment. Dependencies on temperature, density, and magnetic fluctuation level are described. The magnetic fluctuation spectrum is modeled for dissipation associated with viscosity, resistivity and cyclotron resonances. When Visco-resistive dissipation range spectra derived for MHD turbulence are fit to the MST spectrum, the viscosity and resistivity inferred are much larger than the experimental values. Analysis of asymmetry in the toroidal wavenumber spectrum suggests that additional dissipation is coming from the cyclotron resonance with impurity ions.

## 1. Introduction

The anomalous heating of ions observed in the reversed field pinch (RFP) channels magnetic energy associated with electrons to the ion distribution. Because the process is anomalous, the benefits of channeling energy to the ions are offset by electron heat losses. While widely observed [1]-[4], an assessment of tradeoffs and efficiencies has been hindered by lack of a confirmed viable mechanism. A variety of mechanisms have been proposed [5]-[8]. Some have difficulty explaining observations [5]-[6], while for others, comparison with experiment has been inconclusive [7]-[8]. Recent observations indicate that impurity ions play a significant role in anomalous ion heating. During a sawtooth crash impurity temperatures  $T_\alpha$  rise by hundreds of eV to values that satisfy  $T_\alpha > T_i > T_e$  where  $T_i$  is the temperature of the main gas ions, and  $T_e$  is the temperature of the electrons. The rates of heating satisfy a similar inequality,  $\Delta T_\alpha / \Delta t > \Delta T_i / \Delta t > \Delta T_e / \Delta t$ . These observations are similar in many respects to anomalous ion heating in the solar wind and solar corona [9]. The prominence of the role played by impurities, and the widely held view that coronal heating is related to magnetic turbulence, leads us to formulate a theory for ion heating via impurity ion-cyclotron-resonant damping of the turbulent energy cascaded from unstable global tearing modes. The theory extends previous work that treated the fluctuations of the cascade as Alfvén waves [8], but ignored impurities. The theory is based on solution of the plasma dielectric and is shown to yield ion-heating rates that are consistent with experimental observation.

To enable experimental assessment we calculate other observable consequences, including the scaling of heating rates with density, temperature, and magnetic fluctuation level; impurity vs. bulk-ion heating; and collisional effects like temperature isotropization. To study heating rates and collisional effects we introduce a 0-D transport model that includes the wave damping rates on cyclotron resonant impurities, as calculated from the plasma dielectric, loss rates due to turbulent transport, and collisional transfer among impurities, main gas ions, electrons, and perpendicular and parallel temperatures. Taking advantage of new magnetic fluctuation measurements suggesting exponential falloff of fluctuation energy with toroidal wavenumber, we model dissipation range spectra in MHD turbulence,

considering dissipation both from collisional processes and impurity-cyclotron-resonance damping. MHD dissipation range spectra have not been derived previously, despite a number of measurements in magnetic turbulence suggesting a transition to a dissipation range [10]-[12]. We derive dissipation range spectra for MHD, corresponding to both aligned [13] and unaligned [14] turbulence, and for magnetic Prandtl numbers  $Pm \leq 1$ , extending a closure technique from fluid dynamics [15] to magnetic turbulence.

## 2. Energy Flow from Electron to Ion Channels

The strongest increases in ion temperature observed in MST occur as part of a sawtooth crash. Hence we consider ion heating during sawtooth crashes. The crash intensifies the  $m = 1$  spectrum, but the  $m = 0$  resonant surface must be present in the plasma. Heating is not localized to that radius, suggesting involvement of a mode-coupling process with  $m = 0$ . The observations that  $T_\alpha > T_i > T_e$  and  $\Delta T_\alpha / \Delta t > \Delta T_i / \Delta t > \Delta T_e / \Delta t$  indicate that the process preferentially heats impurity ions. These features are consistent with a turbulent cascade involving  $m = 1$  fluctuations that transfer energy to higher toroidal wavenumber  $n$  through coupling to  $m = 0$ . Energy is dissipated to impurity ions by cyclotron resonance. Impurities are resonant at lower frequencies than bulk ions, allowing the greater fluctuation energy at low frequency to drive stronger heating. From the unstable Ohmic current distribution, electron-channel energy flows to the ion channel with quantifiable branching ratios. A portion of the fluctuation energy,  $\epsilon_{inv}$ , is carried to global scales by an inverse helicity cascade that reinforces the Taylor state. The remainder,  $\epsilon_{for}$ , cascades to small scales where it is subject to resonant absorption. The branching ratio is

$$\frac{\epsilon_{for}}{\epsilon_{inv}} = F(k) \frac{V_{anom}}{V_{Sp}} \quad (1)$$

where  $V_{anom}$  and  $V_{Sp}$  are anomalous and classical (Spitzer) loop voltages, and  $F(k)$  is an order-unity function of the equilibrium field configuration. The ratio has a value near 0.7.

## 3. Cyclotron-Resonance Damping

In MST the fluctuations that participate in the toroidal mode number cascade are bound eigenmodes in the strongly sheared equilibrium magnetic field. Their radial structures are localized by shear about the rational surfaces, where  $k_{\parallel} = 0$ , but extend beyond to  $k_{\parallel} \neq 0$ . In the outer half of the plasma, magnetic shear makes  $k_{\parallel}$  primarily a function of the toroidal mode number  $n$ , even though the field is mostly poloidal. Hence, is reasonable to think of the fluctuations, which are ideal away from rational surfaces, as Alfvén waves with  $\omega = k_{\parallel} V_A$ , even though the cascade couples toroidal mode numbers. This picture greatly simplifies the task of calculating cyclotron resonant damping: the limit of the plasma dispersion relation with Alfvén-like dispersion can be evaluated, extracting the imaginary part to recover dissipation. The more realistic alternative, to calculate the cyclotron-resonant dissipation of  $\Delta'$ -negative, nonlinearly excited, shear-localized, small-scale, diamagnetic tearing modes is very difficult, even as a computational problem.

Alfvénic dispersion arises from the  $K_{11}$  component of the dielectric tensor [16]. This component dominates wave dispersion when  $k_{\perp} > k_{\parallel}$  decouples the compressible fast and slow modes. With  $B_0$  in the  $z$  direction and  $k$  in the  $x$ - $z$  plane [ $\mathbf{k} = (\sin\theta, 0, \cos\theta)$ ],  $K_{11}$  is given by

$$K_{11} = 1 + \sum_{s=-\infty}^{\infty} \frac{\omega_{ps}^2}{\omega^2} z_s^\alpha Z(z_s^\alpha) \left( \frac{\omega}{\omega - s\Omega_\alpha} \right) \exp(-\lambda_\alpha) \frac{s^2}{\lambda_\alpha} I_s \quad (2)$$

where  $z_s^\alpha = (\omega - s\Omega_\alpha)/\sqrt{2}k_\parallel v_{\parallel\alpha}$ ,  $s$  is an integer,  $\omega_{p\alpha}$  is the plasma frequency,  $\Omega_\alpha$  is the cyclotron frequency,  $\alpha$  labels impurity species, and  $k = k_\parallel$ . There is no mean flow, and  $I_s(\lambda)$  is a modified Bessel function of argument  $\lambda = k_\perp^2 \rho^2$ , where  $\rho$  is the proton gyroradius,  $\lambda_\alpha = k_\perp^2 \rho^2$ , and  $Z(z) = (1/\sqrt{\pi}) \int dt \exp(-t^2)/(t-z)$  is the plasma dispersion function. Equation (2) simplifies to

$$X^3 = \sum_\alpha Y \omega_{pH\alpha} P_\alpha \sum_{s=-\infty}^{\infty} Z(z_\alpha) \exp(-\lambda_\alpha) \frac{s^2}{\lambda_\alpha} I_s \quad (3)$$

where  $X = ck/\Omega_H$ ,  $Y = \omega/\Omega_H$ ,  $z_\alpha = P_\alpha(Y - s\eta_\alpha)/X$ ,  $\eta_\alpha$  is the impurity charge-to-mass ratio,  $P_\alpha = c/\sqrt{2}v_{\parallel\alpha}$ , and  $\omega_{pH\alpha} = \omega_{p\alpha}^2/\Omega_H^2$ .

Solutions of this expression, obtained numerically, are displayed in Fig. 1. The real part of the frequency [part (a)], indicated by the heavy solid line, is seen to asymptote to  $\omega = kV_A$  (dotted line) for small  $k$ . The thin solid line is the solution of  $c^2k^2/\omega_r^2 = \sum_\alpha \omega_{p\alpha}^2/(\Omega_\alpha^2 - \omega_r^2)$ , a common approximation. The dashed/dotted line is a solution of Eq. (3) with the summation over  $s$  truncated to a single value  $s = 1$ . Solutions with a single value of  $s$  asymptote to  $\Omega_\alpha$  for large  $k$ , whereas the pairings  $s = \pm 1, \pm 2$ , etc., force  $\omega_r$  to zero as  $k \rightarrow \infty$ . The damping rate  $\gamma_i$  is small for low  $k$  where  $\omega_r = kV_A$ . However, it increases as  $\omega_r$  approaches  $\Omega_\alpha$  (resonance), and increases further in the non resonant region where  $k \geq k_{crit}$  and  $\omega_r = 0$ .

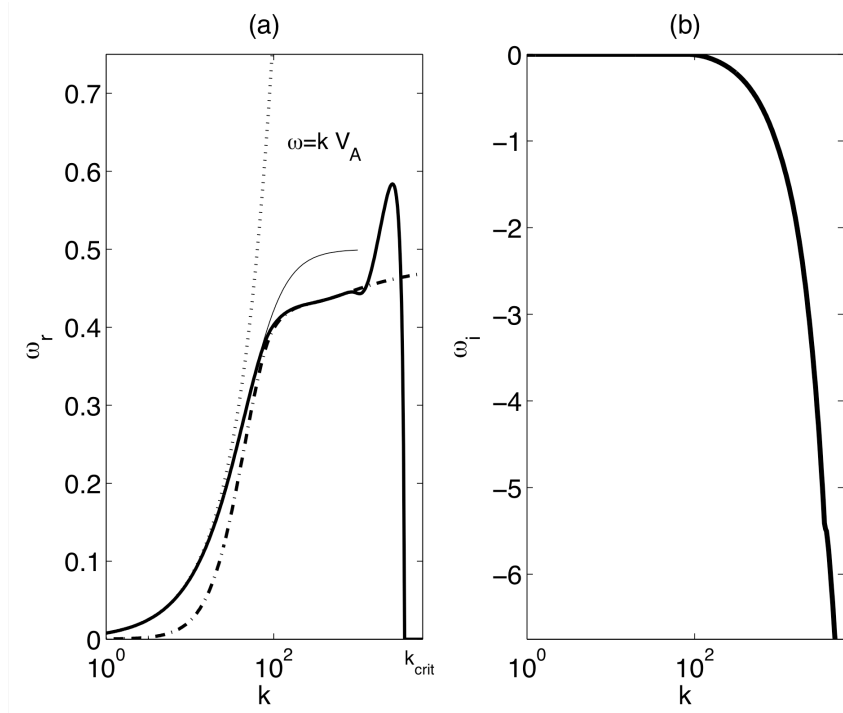


FIG. 1. Real and imaginary parts of wave frequency for damped Alfvén-like waves.

The analytic expression given by the thin solid line in Fig. 1 can be used to calculate the branching ratio for cascade energy deposited in electrons via Landau damping versus an impurity species via cyclotron resonance. The analytic approximation yields a damping rate expression, from which the branching ratio is calculated to be  $\varepsilon_{elec}/\varepsilon_\alpha = (m_e T_\alpha/m_\alpha T_e)^{1/2} k \lambda_D^2 \ll 1$ . The rate at which fluctuation energy is converted to impurity heat via cyclotron absorption is given by  $ndT_\perp/dt = Q_\perp = (\pi a^2)^{-1} (2\pi R)^{-1} \int^{k_{crit}} \gamma_i 4\pi k^2 dk [b^2(k_0)/2\mu_0] (k/k_0)^{-\delta}$ , where  $a$  and  $R$  are the minor and major radii of the torus, and  $b^2(k_0)(k/k_0)^{-\delta}$  is the magnetic fluctuation spectrum (we will take  $\delta = 5/3$ ). This rate is dominated by the larger  $k$  values where  $\omega_r$  deviates from  $\omega_r = kV_A$ . Because we model cascade fluctuations as propagating modes ( $\omega_r \neq 0$ ), we cut off the sum over  $k$  in the heating expression at  $k_{crit}$ . The rates of impurity and bulk-

ion cyclotron heating calculated from the above expressions represent a source in impurity and bulk ion temperature evolution. This source is offset by losses and gains due to collisional equilibration and losses from energy transport out of the system. These sources and sinks form a transport model, whose solution yields impurity and ion temperatures. The transport model solutions, given below, show that there is significant bulk ion heating by collisional transfer from impurities.

#### 4. Impurity Cyclotron Resonance Heating and Consequences

The transport model we employ is a simple 0-D model. We use it to describe the response of ion temperatures to the rise of fluctuation energy in a sawtooth crash. The transport equations include ion-ion collisional equilibration among impurity species and between impurities and bulk ions, electron-ion equilibration, cyclotron damping of fluctuation energy in a prescribed spectrum as given above, and thermal transport via anomalous processes. With appropriate modifications it is also possible to allow for anisotropic temperature and account for anisotropy in the heating rate. Figure 2 shows solutions of the transport model with anisotropic temperature for six regular sawtooth cycles for a carbon impurity species and deuterium bulk ions. The carbon impurity has a large temperature rise. The other temperatures are dependent on collisional equipartition and are smaller. The parallel temperature rise lags in time. Impurity heating rates vary approximately linearly with the magnetic fluctuation level. For the magnetic fluctuation levels of RFPs the heating is significant; for tokamaks it is negligible. Impurity heating rates decrease with increasing temperature. For reactor conditions the rates are more than an order of magnitude lower. Impurity heating rates also increase with decreasing density. In Fig. 2 the deuterium density is  $5 \times 10^{12} \text{ cm}^{-3}$ , and the carbon density 0.1 of the deuterium density. The magnetic fluctuation level is consistent with that of experiment over a sawtooth cycle. If the density is increased to  $10^{13} \text{ cm}^{-3}$  the carbon temperature rise is approximately 100 eV from 50 eV to 150 eV. These values are in experimental ranges.

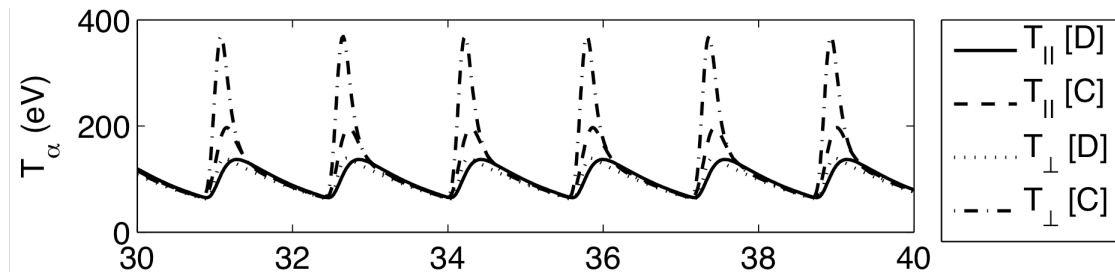


FIG. 2. Responses of impurity [C] and bulk [D] ion temperatures to a sawtooth oscillation in which the fluctuation energy periodically rises and falls. Energy is transferred collisionally from perpendicular to parallel temperature, and from the impurity species to the bulk ion species.

#### 5. Effect on Spectrum I: Visco-resistive Dissipation Range in MHD Turbulence

The significant energy transfer to ions from the magnetic fluctuation spectrum should affect the spectrum shape, imposing a dissipation range. The same statement should also hold for the spectrum of magnetic turbulence in the solar corona and solar wind, provided the energy for coronal heating is extracted from the fluctuation spectrum. However spectra in MST and in the solar wind and solar corona have historically been interpreted as power law spectra, even when the fall off becomes steeper at higher wavenumber. For example, the spectrum in MST has typically been interpreted as a dual-range power law, with spectral indices near  $-5/3$  and  $-4$  in low and high wavenumber ranges. Likewise, solar wind spectra, even in ranges

described as dissipative, are fit with increasingly steep power law exponents [12]. In the case of MST, it appears that an exponential falloff provides a better fit to the spectrum [17]. Exponential spectra for dissipation range turbulence are a staple in Navier-Stokes turbulence, with a number of similar exponential laws having been derived [18]. Surprisingly, it does not appear that dissipation range spectra have been derived for MHD. We address this situation, first deriving dissipation range spectra for viscous and resistive dissipation, and then considering dissipation by cyclotron-resonance absorption.

For MST, the magnetic Prandtl number  $P_m$  is close to unity, hence, we examine the dissipation range for  $P_m=1$ . Using Elsässer variables, the MHD equations can be written as  $\partial \mathbf{Z}_{\pm} / \partial t + \mathbf{Z}_{\mp} \cdot \nabla \mathbf{Z}_{\pm} = -\nabla(p + B^2/2) + \eta \nabla^2 \mathbf{Z}_{\pm}$ , where  $\mathbf{Z}_{\pm} = \mathbf{v} \pm \mathbf{B}$ , and  $\eta$  is the coefficient of dissipation (viscous and resistive). In the inertial range the nonlinearities transfer energy spectrally to higher wavenumber with essentially no loss of energy. In the dissipative range, the nonlinearities continue to transfer energy spectrally, but viscous and resistive energy dissipation rates exceed the nonlinear rates of energy transfer. As a result, energy available for spectral transfer is attenuated as it progresses to successively smaller scales. This is expressed by

$$-2\eta E_{\pm} k^2 = \frac{dT_{\pm}}{dk}, \quad (4)$$

where  $E_{\pm}(k) = \int Z_{\pm}^2 \exp[i\mathbf{k} \cdot \mathbf{x}] d^3x$  is the spectral energy density and  $T_{\pm}(k) = Z_{\pm}^2 Z_{\mp} k \Theta_k$  is the spectral energy transfer rate. In the last expression,  $\Theta_k$  is the alignment factor. If  $\mathbf{Z}_+$  and  $\mathbf{Z}_-$  are perpendicular,  $\Theta_k = 1$ . This orientation maximizes the nonlinearity. In this case, the inertial range spectrum, obtained from  $\varepsilon = T_{\pm}(k)$ , is the Goldreich-Sridhar spectrum  $E_{\pm}(k) = \varepsilon^{2/3} k^{-5/3}$  [14]. In this situation the fields are said to be unaligned. It is postulated that when there is a strong mean field the fields become partially aligned, resulting in  $\Theta_k < 1$  [13]. When  $\Theta_k < 1$  the nonlinearity is partially depleted and spectral transfer is weaker. If  $\Theta_k$  is proportional to  $k^{-1/4}$  the reduction recovers the inertial range spectrum originally proposed by Iroshnikov and Kraichnan (IK) [19]-[20],  $E_{\pm}(k) = \varepsilon^{1/2} V_A^{1/2} k^{-3/2}$ , where  $V_A = B_0 / (4\pi\rho)^{1/2}$ . Unlike IK the fluctuations in aligned turbulence are anisotropic. Not only are they stretched along the field line, as is also the case when  $\Theta_k = 1$ , but they are oblate in the plane perpendicular to the mean field. The oblate shape creates the partial alignment responsible for depleting the nonlinearity. The postulated alignment explains numerical simulations that reproduce the IK spectrum when there is a strong mean field [21]. Alignment has recently been observed directly in simulations [22].

To obtain dissipation range spectra it is necessary to close the expression for the spectral energy transfer rate,  $T_{\pm}(k) = Z_{\pm}^2 Z_{\mp} k \Theta_k$ , so that it is expressed in terms of  $E_{\pm}$ . Substitution into Eq. (4) then yields a differential equation that can be solved for the spectrum. A closure procedure given by Tennekes and Lumley (TL) for Navier-Stokes turbulence [15] is adaptable to MHD for magnetic Prandtl numbers  $P_m$  of unity or lower [17]. The closure results in MHD dissipation range spectra that are physically meaningful because: 1) physically meaningful Kolmogorov wavenumbers, corresponding to the scale at which the inertial and dissipative forces balance, are recovered; 2) the spectra asymptote to MHD inertial range spectra for wavenumbers that are smaller than the Kolmogorov wavenumber; and 3) the closure can accommodate both aligned and unaligned turbulence while still satisfying the first two conditions. The last condition suggests that the filament-like structures of aligned turbulence and the sheet-like structures of unaligned turbulence can both carry into the dissipation range as dissipative structures. The TL procedure also handles turbulence with  $P_m < 1$ , yielding distinct spectra for the magnetic and fluid energies that

satisfy the first two conditions. For  $\text{Pm} > 1$  the transfer rates that govern the dissimilar spectra for magnetic field and flow are represented by the same heuristic form. Consequently TL cannot be extended to MHD for  $\text{Pm} > 1$  without more detailed modeling of the turbulent stresses that govern  $T$ .

For unaligned turbulence, the TL procedure replaces the factor  $Z_{\pm}^2$  in  $T_{\pm}(k)$  with  $E_{\pm}(k)k$ , and the factor  $Z_{\mp}$  with  $\varepsilon^{1/3}/k^{2/3}$ . The latter is the inertial range amplitude obtained from the inertial Obukov balance  $\varepsilon = T_{\pm}(k) = Z_{\pm}^2 Z_{\mp} k \Theta_k = Z_{\mp}^3 k$ . These two replacements give  $T_{\pm} = E_{\pm}(k) \varepsilon^{1/3} k^{5/3}$ , and together constitute the TL closure. Substitution into Eq. (4), and solution of the differential equation yield the following spectra

$$E_{\pm}(k) = a\varepsilon^{2/3} k^{-5/3} \exp\left[-\frac{3}{2}\left(\frac{k}{k_{\eta_{un}}}\right)^{4/3}\right], \quad (\text{unaligned}) \quad (5)$$

where  $k_{\eta_{un}} = \varepsilon^{1/4}/\eta^{3/4}$  is recognizable as the Kolmogorov wavenumber for turbulence whose inertial spectrum decays as  $k^{-5/3}$ .

For aligned turbulence the closure is applied to  $T_{\pm}(k) = Z_{\pm}^2 Z_{\mp} k \Theta_k$ , with  $\Theta_k$  different from unity. As before  $Z_{\pm}^2 = E_{\pm}(k)k$ . The  $k$  dependence of  $\Theta_k$  is chosen so that  $\varepsilon = T_{\pm}(k) = Z_{\pm}^2 Z_{\mp} k \Theta_k = E_{\pm}^{3/2} k^{5/2} \Theta_k$  yields the IK spectrum  $E_{\pm}(k) = \varepsilon^{1/2} V_A^{1/2} / k^{3/2}$ . This gives  $\Theta_k = \varepsilon^{1/4} / V_A^{3/4} k^{1/4}$ . The remaining factor  $Z_{\mp}$  is taken from the IK spectrum with  $E_{\pm}(k) = Z_{\mp}^2 / k = \varepsilon^{1/2} V_A k^{-3/2}$ , or  $Z_{\mp} = \varepsilon^{1/4} V_A^{1/4} / k^{1/4}$ . With these substitutions for  $Z_{\pm}^2$ ,  $\Theta_k$ , and  $Z_{\mp}$ ,  $T_{\pm}(k) = E_{\pm}(k) \varepsilon^{1/2} k^{3/2} / V_A^{1/2}$ . This expression constitutes the closure. It is substituted into Eq. (4), which in turn is solved to yield the dissipation range spectrum for aligned turbulence:

$$E_{\pm}(k) = a\varepsilon^{1/2} V_A^{1/2} k^{-3/2} \exp\left[-\frac{4}{3}\left(\frac{k}{k_{\eta_{al}}}\right)^{3/2}\right], \quad (\text{aligned}) \quad (6)$$

where  $k_{\eta_{al}} = \varepsilon^{1/3} / V_A^{1/3} \eta^{3/2}$  is the Kolmogorov wavenumber for aligned turbulence. From the functional forms of Eqs. (5) and (6) it is evident that, whereas the aligned spectrum is broader than the unaligned spectrum in the inertial range, it has a steeper exponential decay in the dissipation range. This feature has a simple explanation. It can be shown that the powers of  $k$  in the exponential argument can be recovered from a determination of the amount of energy lost to dissipation in an inertial eddy turnover time. In the aligned case the broader inertial range spectrum results from the depletion of the nonlinearity, which in turn gives a longer eddy turnover time. But the longer eddy turnover time allows greater dissipation over the timescale of nonlinear energy transfer. Hence, aligned turbulence has steeper decay in the dissipation range.

The spectra of Eqs. (5) and (6) have two parameters,  $a$  and  $k_{\eta}$ . These parameters can be determined by fitting to observed spectra. When this is done for the MST spectrum, the resistivity from the fit is approximately  $50 \text{ m}^2/\text{s}$ , several orders of magnitude larger than the true resistivity. This indicates that there is another dissipation mechanism that is much stronger than resistivity. Since this analysis properly accounts for spectral transfer, the enhanced dissipation must correspond to some other loss of spectral energy. The considerations of Secs. 2 - 4 point to cyclotron-resonant absorption as a likely candidate for this loss.

## 6. Effect on Spectrum II: Impurity-Cyclotron-Resonance Dissipation Range

In accordance with the above conclusion, we seek some visible signature of cyclotron-resonant absorption in the magnetic fluctuation spectrum of MST. The left hand portion of figure 3 shows the spectrum as a function of toroidal wavenumber  $n$ . There is a pronounced

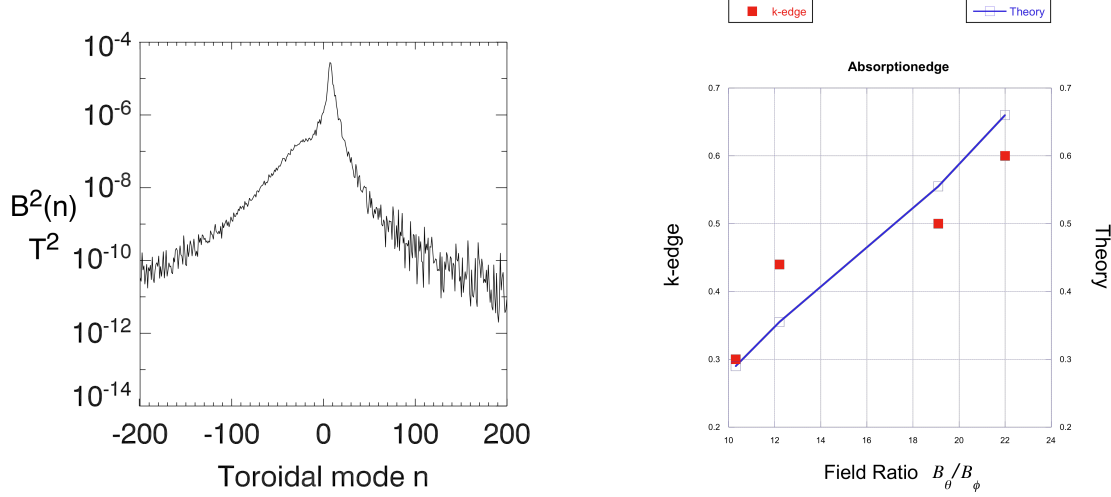


FIG. 3. On the left, toroidal mode number spectrum in MST, showing deficit of energy on the positive- $n$  side. On the right, scaling of deficit wavenumber with ratio of poloidal to toroidal field. The agreement of theory and experiment suggests that the deficit is associated with cyclotron resonant absorption of fluctuation energy.

asymmetry associated with a deficit of energy on the positive- $n$  side of the spectrum. We investigate the possibility that the deficit is due to cyclotron-resonant absorption. Note first that in an impurity cyclotron resonance with Alfvén waves  $\omega = k_{\parallel} V_A = \Omega_{\alpha}$  the resonance occurs for one sign of the wavenumber only. We use this condition to determine a wavenumber at which cyclotron absorption begins to affect the spectrum. In a torus with a sheared magnetic field, the parallel wavenumber depends on the toroidal field  $B_\phi$  and poloidal field  $B_\theta$  as follows:  $k_{\parallel}(r) = \mathbf{k} \cdot \mathbf{B}/B = m/r - nB_\theta(r)/RB_\phi(r)$ . Here we restrict ourselves to the outer part of the plasma where  $B_\theta \gg B_\phi$ . For the canonical toroidal mode number cascade invoked in Secs. 2-4, we set  $m = 1$ , and find the value of  $n/R$  for which  $k_{\parallel} V_A = \Omega_{\alpha}$ , where  $\Omega_{\alpha} = \Omega_H Z/\mu$  is an impurity cyclotron frequency, and can be expressed in terms of the hydrogen cyclotron frequency  $\Omega_H$ , charge number  $Z$ , and mass factor  $\mu$  relative to the hydrogen mass. This defines a wavenumber  $k_{edge}$  at which cyclotron absorption begins to affect the spectrum,

$$k_{edge} = \frac{n}{R} = \frac{B_\theta(r)}{B_\phi(r)} \left[ \frac{1}{r} - \Omega_H \frac{Z}{\mu} V_A \right]. \quad (7)$$

In a sheared field  $k_{edge}$  changes with minor radius because the ratio  $B_\theta(r)/B_\phi(r)$  changes with minor radius. We pick a nominal  $k_{edge}$  from the spectrum in Fig. 3 as the wavenumber at which the intensity falls below some threshold, and then track how  $k_{edge}$  varies with  $B_\theta(r)/B_\phi(r)$  as the probe is placed at different values of the minor radius. The results are shown in the right hand side of Fig. 3 as the closed square boxes. The line connecting open boxes is the theoretical expression from Eq. (7). It is evaluated for  $Z/\mu = 0.38$ , corresponding to a low value of  $\Omega_{\alpha}$  in this case for the impurity  $O^{+6}$ . The overlap of the theoretical and experimental results is not significant, because the intensity threshold defining  $k_{edge}$  in the spectrum was arbitrarily chosen. However, the agreement of the slopes is significant, and

indicates that the observed asymmetrical deficit of energy in the spectrum is sensitive to the cyclotron resonance condition  $k_{\parallel}V_A = \Omega_{\alpha}$ . This indicates there is a causal link between elevated ion temperatures and the fluctuation spectrum, providing new evidence that ion heating in the RFP is related to cyclotron resonant absorption of fluctuation energy. In the future it will be important to develop improved analyses of resonant absorption that account for the fluctuations as internally resonant modes in a sheared field, and that properly treat the asymmetry of absorption in parallel wavenumber.

## 7. Conclusions

Observations of anomalous ion heating in the RFP have been difficult to understand in detail, in part, because there has been a large number of mechanisms proposed, but insufficient point-of-contact between theory and experiment to confirm or falsify hypotheses. This work reports progress in the case of cyclotron-resonant absorption of magnetic fluctuation energy. The mechanism is shown to give heating rates that are broadly consistent with experiment, while also accounting for energy partition between impurities and the bulk ion species in a sawtooth crash. Dependencies on density, temperature and fluctuation intensity are also consistent with RFP phenomena. The spectrum shows dissipation that cannot be accounted for by resistivity and viscosity, but is consistent with cyclotron-resonant absorption.

Work supported by USDOE under the grant DE-FG02-85ER53212.

- [1] SCIME, E., et al., Phys. Fluids B **4** (1992) 4062.
- [2] JONES B. and WILSON R., Nuclear Fusion (1962) 889.
- [3] HOWELL, R.B. and NAGAYAMA, Y., Phys. Fluids **28** (1985) 743.
- [4] SASAKI, K., et al., Plasma Phys. Controlled Fusion **39** (1987) 333.
- [5] YOSHIDA, Z., Nuclear Fusion **31** (1991) 386.
- [6] McCHESNEY, J.M., et al., Phys. Rev. Lett. **59** (1987) 1436.
- [7] GATTO, R. and TERRY, P.W., Phys. Plasmas **8** (2001) 825.
- [8] MATTOR, N., et al., Comments Plasma Phys. Controlled Fusion **15** (1992) 65.
- [9] CRANMER, S.R. and VAN BALLEGOOIJEN, A.A., Astrophys. J. **594** (2003) 573.
- [10] LEAMON, R.J., et al., J. Geophys. Res. **103** (1998) 4775.
- [11] SMITH, C.W., et al., Astrophys. J. Lett. **645** (2006) L85.
- [12] CHASTON, C.C., et al., Phys. Rev. Lett. **100** (2008) 175003.
- [13] BOLDYREV, S., Astrophys. J. Lett. **626** (2005) L37.
- [14] GOLDREICH, P. and SRIDHAR, S., Astrophys. J. **443** (1995) 763.
- [15] TENNEKES, H. and LUMLEY, J.L., A First Course in Turbulence (MIT Press, Cambridge, MA, 1972).
- [16] TANGRI, V., TERRY, P.W., and FIKSEL, G., Phys. Plasmas, submitted.
- [17] TERRY, P.W., TANGRI, V., and BAVER, D.A., Phys. Plasmas, submitted.
- [18] SMITH, L.M. and REYNOLDS, W.C., Phys. Fluids A **3** (1991) 392.
- [19] IROSHNIKOV, P.S., Soviet Astron. **7** (1964) 566.
- [20] KRAICHNAN, R.H., Phys. Fluids **8** (1965) 1385.
- [21] BISKAMP, D. and MÜLLER, W.-C., Phys. Plasmas **7** (2000) 4889.
- [22] MASON, J., CATTANEO, F., and BOLDYREV, S., Phys. Rev. Lett. **97** (2007) 255002.